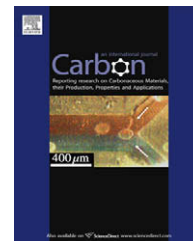


available at [www.sciencedirect.com](http://www.sciencedirect.com)journal homepage: [www.elsevier.com/locate/carbon](http://www.elsevier.com/locate/carbon)

# Platinum nanoparticles supported on stacked-cup carbon nanofibers as electrocatalysts for proton exchange membrane fuel cell

Wenzhen Li <sup>\*</sup>, Mahesh Waje <sup>a</sup>, Zhongwei Chen <sup>b</sup>, Paul Larsen, Yushan Yan <sup>\*</sup>

Department of Chemical and Environmental Engineering and College of Engineering, Center for Environmental Research Technology (CE-CERT), University of California, Riverside, CA 92521, USA

## ARTICLE INFO

### Article history:

Received 30 September 2009

Accepted 5 November 2009

Available online 11 November 2009

## ABSTRACT

Inexpensive stacked-cup carbon nanofibers (SC-CNFs) supported Pt nanoparticles with a loading from 5 to 30 wt.% were prepared through a modified ethylene glycol method. XRD and TEM characterizations show that the average Pt particle sizes increase with increasing metal loading, and they can be controlled <5 nm with a uniform dispersion. A self-developed filtration process was employed to fabricate Pt/SC-CNFs film-based membrane electrode assembly (MEA), and the catalyst transfer efficiency can reach nearly 100% using a super-hydrophobic polycarbonate filter. The thickness of catalyst layer can be accurately controlled through altering Pt loadings of the catalyst and electrode, this is in good agreement with our theoretical calculation. For Pt/SC-CNFs-based-MEAs, Pt cathode loading was found more critical than Pt anode loading on proton exchange membrane fuel cell (PEMFC) performance. The Pt/SC-CNFs-based MEA with an optimized 50 wt.% Nafion content demonstrates higher PEMFC performance than the carbon black-based MEA with an optimized 30 wt.% Nafion content. SC-CNFs possess much larger length-to-diameter ratio than carbon black particles, it makes Pt/SC-CNFs more easily form continuously conductive networks in the Nafion matrix than carbon black. Therefore, the Pt/SC-CNFs-based MEA demonstrates higher Pt utilization than carbon black-based MEA, which implies possible reduction in Pt loading of MEA.

© 2009 Elsevier Ltd. All rights reserved.

## 1. Introduction

Working at low temperature (<90 °C), hydrogen fueled proton exchange membrane fuel cells (PEMFCs) have been identified as being promising for powering autos, houses and electronics [1]. However, compared to the fast hydrogen oxidation reaction (HOR) taken at the anode, oxygen reduction reaction (ORR) taken at the cathode is a highly irreversible, complex,

four-electron-transferred reaction, and its kinetics is very sluggish. Even at the most active Pt catalyst surface, the exchange current density of ORR is  $10^{-9}$  A/cm<sup>2</sup>, which is 6 magnitudes higher than HOR ( $10^{-3}$  A/cm<sup>2</sup>). Under open circuit state (OCV), the over-potential of ORR is >200 mV at the Pt surface, this substantially reduces the thermodynamics energy conversion efficiency [2–3]. The state-of-the-art membrane electrode assembly (MEA) has a Pt metal loading of

<sup>\*</sup> Corresponding authors: Present address: Department of Chemical Engineering, Michigan Technological University, 1400 Townsend Drive, Houghton, MI 49931, USA. Fax: +1 906 487 3132 (W. Li), fax: +1 951 827 8648 (Y. Yan).

E-mail addresses: [wzli@mtu.edu](mailto:wzli@mtu.edu) (W. Li), [yushan.yan@ucr.edu](mailto:yushan.yan@ucr.edu) (Y. Yan).

<sup>a</sup> Present address: Lynntech Inc., 7610 Eastmark Dr. College station, TX 77840, USA.

<sup>b</sup> Present address: Department of Chemical Engineering, Nanotechnology Institute and Waterloo Institute for Sustainable Energy, University of Waterloo, 200 University Avenue West, Waterloo, Ontario, Canada N2L 3G1.

0008-6223/\$ - see front matter © 2009 Elsevier Ltd. All rights reserved.

doi:10.1016/j.carbon.2009.11.017

0.6–0.8 mg/cm<sup>2</sup><sub>MEA</sub>, at a working voltage of 0.65 V, the typical current density is around 1.0 A/cm<sup>2</sup>, this equals to a specific power density of 0.7 W/cm<sup>2</sup><sub>MEA</sub>, which could be translated into 0.85–1.1 g<sub>Pt</sub>/kW. In order to meet the target for large scale automobile application of < 0.2 g<sub>Pt</sub>/kW at fuel cell working voltage of > 0.65 V, there should be a 5-time-fold Pt reduction both for the reason of cost and noble metal supply limitation [3].

Three approaches to improving Pt mass activity and/or reducing Pt loading have been actively studied in recent years: The first one is alloying Pt with a second base metal (M = Fe, Co, Ni, Cu, etc.) to improve the Pt intrinsic activity towards ORR [3–11]. GM researchers have shown that the target of 0.2 g<sub>Pt</sub>/kW at cell operation voltage of 0.65 V is viable and can be accomplished by reducing the currently observed mass transport loss by 50%, together with implementing Pt-alloy catalyst (e.g., Pt–Co) with a 2–4-fold increased mass activity over the state-of-the-art Pt/C catalysts [3]. This means a reduction in the Pt loading to ca. 1/4 of current Pt loading in MEAs cathode, from about 0.4–0.1 mg/cm<sup>2</sup> without a loss in cell voltage, while still maintaining maximum power density and cell efficiency. The hypotheses of the ORR mass activity enhancement in Pt-alloy over Pt have also been proposed and can be classified broadly as structural factors [4], electronic factors [5–6], inhibition by anion adsorption [9], surface sensitive factors: formation of a unique Pt ‘skin-layer’ structure [10], and ‘H<sub>2</sub>O<sub>2</sub> decomposition’ mechanisms [11]. However, a general concern with Pt–M alloy as acid electrolyte fuel cell catalyst is the leaching of base metal M, which was suggested to raise the following problems of (a) cathode catalytic activity degradation, (b) reduction in membrane conductivity due to metal ionic contamination, and (c) cathode catalyst layer resistance increase [3].

The second approach is to investigate non-noble metal catalysts [12–22], and it can be generally categorized into three classes, (1) macrocyclic complexes, i.e., porphyrins or phthalocyanines [13–16], (2) metal carbides/nitrides [17], and (3) transition metal chalcogenides (e.g., ruthenium-based chalcogenides) [18–19]. Recently, researchers in Los Alamos national laboratory developed a new class of non-precious catalyst, based on cobalt–polypyrrole–carbon (Co–PPY–C), which shows an encouraging durability (≈100 h) [20]. Dodelt’s group reported micro carbon supported Fe-based catalysts show equal ORR activity as Pt/C with 0.4 mgPt/cm<sup>2</sup> at a cell voltage of ≥ 0.9 V [21]. Nitrogen doped aligned carbon nanotube demonstrates higher ORR activity in alkaline electrolyte [22]. However, great breakthrough in the areas of materials and technology are still need to improve intrinsic activity and life-time of non-precious metal based electrocatalysts.

The third approach to improving Pt mass activity and durability is to study carbon nanomaterials as electrocatalyst support [23–40]. Carbon nanotubes (CNTs), a new type of carbon allotrope consisting of helical curved hexagonal graphite sheets, have attracted great interest from both fundamental and applied points of view since their discovery and large scale synthesis have been explored, owing to their high mechanical and unique electronic properties [41,42]. These CNTs materials are considered to be potentially useful electrocatalysts support for fuel cell [26,27,29,30,32–39]. Other carbon nanomaterials, such as carbon tubule membrane [23],

highly ordered nanoporous carbon [24], carbon nanohorns [28], carbon nanocoils [31] supported Pt/PtRu nanoparticles were also found to have higher ORR or MOR activity than traditional carbon black, e.g., Vulcan XC-72R, Ketjen carbon black and black pearl 2000. However, these CNTs are relatively expensive (e.g., \$20–50/g for multi-walled carbon nanotubes, MWNTs) today and are not considered economically viable for large scale transportation applications. To overcome the cost barriers, we have identified a type of one dimensional (1-D) carbon nanomaterial – stacked-cup carbon nanofibers (SC-CNFs) [40], which can be inexpensive (e.g., \$0.01–0.02/g) and produced on large scale (e.g., 10,000 lbs/yr currently with easy scale-up). Although SC-CNFs are still more expensive than carbon black, its cost is negligible when compared to Pt (\$47/g), making it a viable support material. Further, the stacked-cup layer structure is expected to anchor Pt nanoparticles, which could offer a longer durability compared to common smooth surface tube-morphology.

In this paper, we prepared SC-CNFs supported Pt nanoparticles using a self-developed ethylene glycol (EG) synthesis method [26,29]. XRD and TEM were conducted to determine the Pt particle size and size distribution. The catalyst coated membrane (CCM) was prepared by a self-developed filtration method [36], by which uniform thin catalyst film and nearly 100% catalyst transfer efficiency could be attained. Theoretical calculations were used to predict the maximum Pt loading in the catalysts and the thickness of catalyst layers. The PEM single cell performances of the MEAs with Pt/SC-CNFs with different Pt loadings (in catalyst and electrode) were investigated. The electrode structures for the MEAs with Pt/SC-CNFs and conventional carbon black (C) supported catalysts were further optimized.

## 2. Experimental

### 2.1. Catalysts preparation and characterization

Inexpensive SC-CNFs were provided by Applied Science Corp and produced by a chemical vapor deposition (CVD) approach. Most SC-CNFs have a diameter of 75–100 nm and their surface area is approximately 100 m<sup>2</sup>/g. In the aim of creating more functional groups on the outer walls of SC-CNFs, the as-received SC-CNFs sample in the experiments was pre-oxidized by an acid mixture of 2.0 M H<sub>2</sub>SO<sub>4</sub>–4.0 M HNO<sub>3</sub> for 6 h under refluxing condition at 100 °C.

Pt/SC-CNFs catalysts were prepared by a modified EG reduction method [29]. The preparation method is briefly described as follows: the surface oxidized SC-CNFs (226 mg) were suspended in an EG solution and treated in an ultrasonic bath to form an ink. Then an EG solution of hexachloroplatinic acid was added drop wise, under vigorously stirring conditions for 2 h. A solution of 1.0 M NaOH in EG was added to adjust the pH of the synthesis solution to above 13, and then the mixture was heated at 140 °C for 3 h to reduce the Pt completely. After cooling down to room temperature, the pH of the synthesis system was adjusted to 2–3 by 0.1 M HCl. The whole preparation process was conducted under flowing argon. After filtration (filter paper: Whatman, Grade 1), washing, and drying in vacuum at 80 °C for 8 h, the Pt/SC-CNFs catalysts

were finally obtained. The filtrated solvent was transparent with a color of pale yellow, and the weight calculation showed the Pt conversion was nearly 100% during the synthesis process, the catalyst metal loading varied from 5 wt.%, 10 wt.%, 20 wt.% to 30 wt.%. A 20 wt.% Pt/C catalyst was kindly provided by BASF-Fuel Cell and used as a control sample.

Pt/SC-CNFs powders were characterized by X-ray diffraction (XRD) using Cu-K $\alpha$  radiation with a Ni filter. The tube current was 40 mA with a tube voltage of 40 kV. The  $2\theta$  regions between  $20^\circ$  and  $85^\circ$  were explored at a scan rate of  $5^\circ/\text{min}$ . Transmission electron microscopy (TEM) was conducted on a PHILIPS S3000 operating at 300 kV to get the information of Pt particle size and size distribution.

## 2.2. Theoretical calculations

We made theoretical calculations on the maximum possible Pt loading on CNFs and the thicknesses of catalyst layers. We assumed the porosity of catalyst layer was 0.3, the average distance between two Pt particles was twice as the Pt diameter (based on TEM images), the fraction of surface was covered by Pt nanoparticles as a function of arrangement (0.7732 for triangular close packed arrangement), and CNFs packed compactly on the surface of Nafion membrane. Average diameters of CNFs and Pt nanoparticles (e.g., 100 nm for CNFs and 2.5 nm for Pt nanoparticles) were used for calculations on the thickness of catalyst layer. The other constants were:  $21,500 \text{ kg/m}^3$  for Pt density,  $2000 \text{ kg/m}^3$  for carbon density,  $2100 \text{ kg/m}^3$  for Nafion density. Therefore, we can obtain the maximum possible Pt loading for a given diameter CNFs supported Pt nanoparticles with fixed size, and the catalyst

layer thickness of the Pt/SC-CNFs with a given fiber diameter and Pt catalyst loading.

## 2.3. MEA fabrication and characterization

A PEMFC's MEA consists of two commercial gas diffusion layers (GDL, 25CC, SGL Corp.) as both anode and cathode substrates, and a catalyst coated membrane (CCM). For preparation of the CCM, we modified a self-developed filtration method to make compact Pt/CNTs films onto both sides of Nafion membrane as anode and cathode catalyst layers [36]. The schematic illustration of the fabrication process is shown in Fig. 1, Pt/SC-CNFs suspension in ethanol with known catalyst quantity was drawn through a  $0.2\text{-}\mu\text{m}$ -pore polycarbonated filter paper. After filtration, a 5 wt.% Nafion<sup>®</sup> solution was used to spray on the surface of the filtrated Pt/SC-CNFs solid, the Nafion weight ratio was altered from 30 wt.% to 50 wt.% for cathode and was constant 50 wt.% for anode. The filtrated Pt/SC-CNFs catalysts were transferred onto Nafion<sup>®</sup> 112 membrane by hot-pressing two catalyst coated sides of the filters onto the Nafion<sup>®</sup> membrane to produce a CCM. The cathode Pt loading is  $0.10 \text{ mg/cm}^2$  and  $0.20 \text{ mg/cm}^2$ , while the anode catalysts loading is from  $0.025 \text{ mgPt/cm}^2$ ,  $0.05 \text{ mgPt/cm}^2$  to  $0.20 \text{ mgPt/cm}^2$ , respectively. Nylon filter was also used to make a MEA to study the influence of filter's surface properties on the 'catalyst transfer efficiency'. A digital cameral Canon SD500 was used to take pictures on the surfaces of blank Nylon and polycarbonated filters, and of the catalyst side of two filters after the transfer process. Pt/C catalyst (20 wt.%, BASF-Fuel Cell) with different Nafion ratio ranging from 15 wt.%, 30 wt.% to 50 wt.% were brushed di-

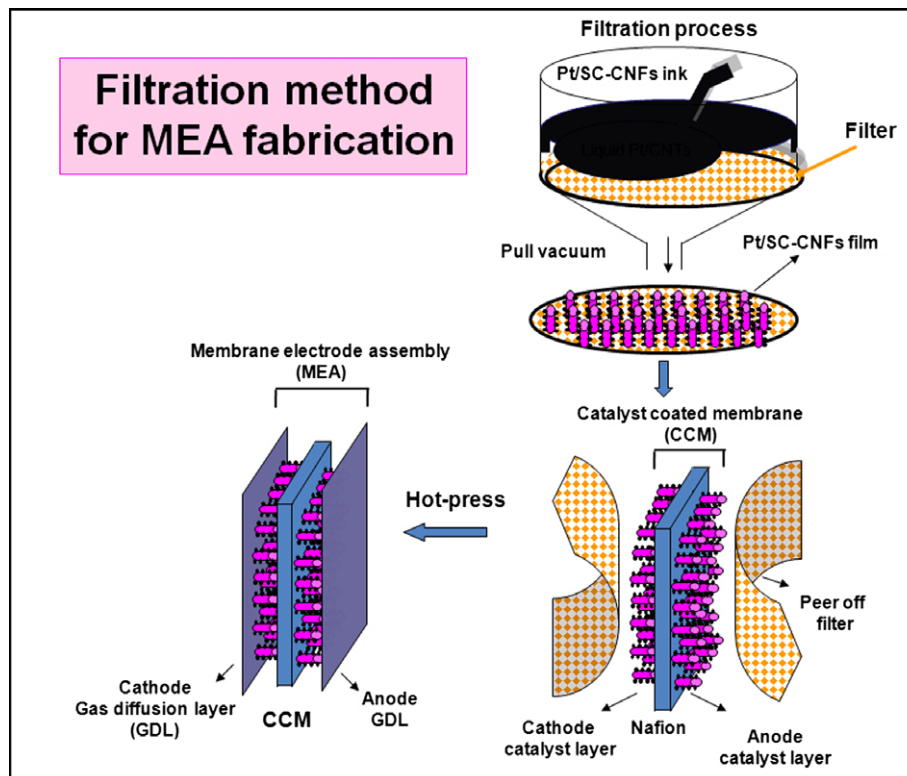


Fig. 1 – Schematic illustration of filtration method for fabricating SC-CNFs based MEA.

rectly on GDL (25CC, SGL) to prepare conventional anode and cathode samples.

Scanning electron microscopy (SEM) was conducted on a PHILIPS XL30-FEG with an operating voltage of 10 kV to study the morphology of the cross-sections of CCMs. The CCM samples were obtained by vertically cutting the electrodes by using a sharp blade, and they were bonded compactly on a 45°-holder with conductive tapes for SEM measurements.

#### 2.4. Fuel cell measurement

The SC-CNFs based MEAs with an active electrode area of 4.4 cm<sup>2</sup> (2.1 cm × 2.1 cm) were obtained by hot-pressing a cathode diffusion layer, a CCM and an anode diffusion layer with a pressure of 50 kg/cm<sup>2</sup>, at 135 °C for 3 min. For comparison, MEAs with Pt/C catalysts with a metal loading of 0.2 mg/cm<sup>2</sup> for both anode and cathode were also fabricated by hot-pressing a conventional anode, cathode and a Nafion® 112 membrane by using same hot-press conditions as described above. The PEMFC performances of these MEAs were measured using an Arbin fuel cell test stand. The operation conditions are described as follows: The oxygen and hydrogen operating pressure was 35 Psi, and their flow rate was 200 mL/min, the temperatures of cell, anode and cathode humidifier were 70 °C, 75 °C and 75 °C, respectively. The I–V curves were collected after a 2-h-activation-process at constant operation voltage of 0.6 V.

### 3. Results and discussion

Carbon nanofibers (CNFs) are cylindrical or conical structures that have diameter from a few to hundreds of nanometers varying from a few to hundreds of nanometers and lengths ranging from less than a micron to millimeters [43,44]. The morphology of CNFs can be categorized into three types: platelet, ribbon and stacked-cup [25]. In this article, we chose SC-CNFs, consisting of stacked curved graphite layers that form cones or cups, which is often referred as a bamboo type, resembling the compartmentalized structure of a bamboo stem, as shown in Fig. 2. Our motivation of choosing SC-CNFs comes from its inexpensive cost and the stacked-cup surface morphology, which is believed to be able to anchor Pt nanoparticles, thus improving the catalyst durability.

The powder XRD patterns for the Pt/SC-CNFs catalysts with metal loading of 5 wt.%, 10 wt.%, 20 wt.% and 30 wt.% are shown in Fig. 3. The strong diffraction peaks observed at 26.5°, 42.4°, 52.7° are attributed to the hexagonal graphite structure (0 0 2), (1 0 0) and (0 0 4), respectively, which reflects SC-CNFs have a high graphite structure and good electrical conduction. With the Pt metal loading increasing, the intensity of diffraction peaks decreases, this means more metal deposition affects the symmetry of graphite structure. The diffraction peaks at  $2\theta = 39.7^\circ$ ,  $46.2^\circ$ ,  $67.4^\circ$  and  $81.2^\circ$  could be assigned to Pt (1 1 1), Pt (2 0 0), Pt (2 2 0) and Pt (3 1 1), respectively. The analysis of Pt diffraction peaks shows that all catalysts have a Pt face centered cubic (fcc) crystal structure. The isolated Pt (2 2 0) peaks were chosen to calculate the average Pt crystalline particle sizes for all the Pt/SC-CNFs samples using the Debye–Scherrer formula, and they were

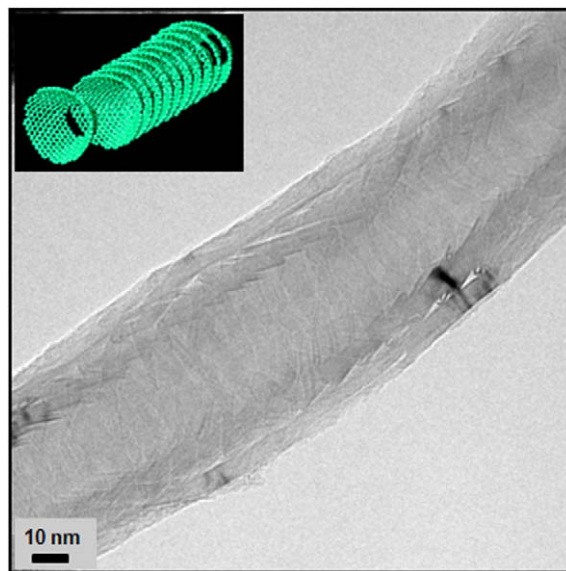


**Fig. 2 – TEM image of SC-CNFs in this study, top-left inserted: illustration of SC-CNFs structure from [45].**

about 2.7 nm for the 30 wt.% sample and 2.4 nm for the 20 wt.% sample. For the Pt/SC-CNFs with metal loading of 5 wt.% and 10 wt.%, the Pt (2 2 0) peaks are very broad, thus meaningful Pt average particle size could not be obtained. The Pt particle sizes are smaller than 2.0 nm. It is well known that Pt particle size gets larger as the ratio of Pt particles to support (catalyst metal loading) increases [7]. Since the support SC-CNFs used in this work have diameters around 75–100 nm, which offers a relatively low surface area of ca. 100 m<sup>2</sup>/g, so the catalyst metal loading plays an important role on the mean particle size [7].

Typical TEM images of the Pt/SC-CNFs catalysts are shown in Fig. 4. For the Pt/SC-CNFs catalysts with 5 wt.%, 10 wt.% and 20 wt.%, small Pt nanoparticles with diameter from 2 to 3 nm are uniformly dispersed onto SC-CNFs outer walls. It can be observed that the metal distribution density becomes higher with metal loading increasing. This is consistent with the XRD results. Minor agglomerations of Pt nanoparticles were observed for the 30 wt.% sample, due to low surface area of the SC-CNFs and high metal loading of 30 wt.% of Pt/SC-CNFs catalyst. We made theoretical calculations to assess the maximum possible Pt loading on the SC-CNFs outer walls, as shown in Fig. 5. It is well known that the Pt mean particle size and SC-CNFs diameters determine the maximum Pt loading. In general, larger Pt particles have smaller total metal surface area, and larger diameter SC-CNFs support offers smaller surface area for residing Pt metal particles. e.g., if the average Pt particle size is as large as 5.0 nm, the SC-CNFs with a diameter of 200 nm can support 28 wt.% Pt nanoparticles, while the SC-CNFs with a diameter of 25 nm can even support 85 wt.% Pt nanoparticles (see the purple curve in Fig. 5). Only 15 wt.% of Pt nanoparticles with an average size of 2.5 nm can be deposited on the SC-CNFs with a diameter of 200 nm, while 50 wt.% Pt nanoparticles with such size (2.5 nm) can be on the SC-CNFs with a larger diameter of 25 nm. In our study, the mean diameter of SC-CNFs is about 100 nm, which is able to reside maximum 22 wt.% and 27 wt.% Pt nanoparticles with



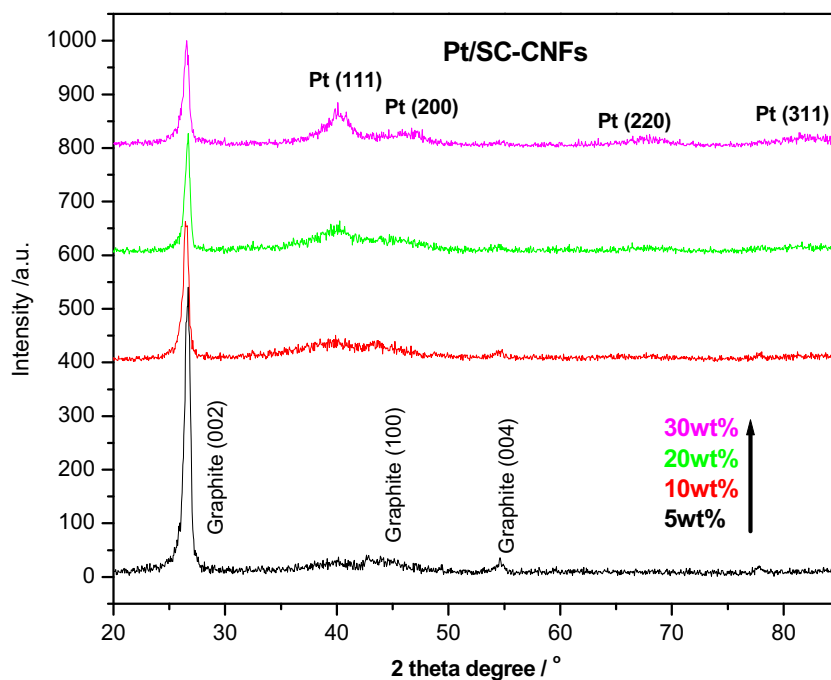


Fig. 3 – XRD patterns of Pt/SC-CNFs with 5 wt.%, 10 wt.%, 20 wt.% and 30 wt.% metal loading.

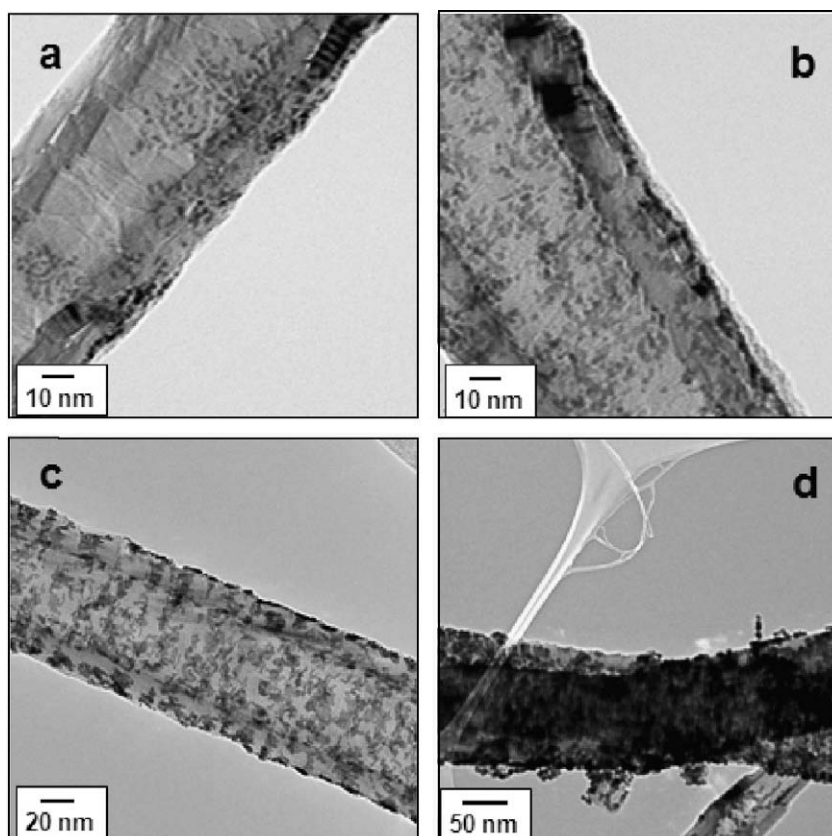


Fig. 4 – TEM images of Pt/SC-CNFs with (a) 5 wt.%, (b) 10 wt.%, (c) 20 wt.% and (d) 30 wt.% metal loading.

average size of 2.5 nm and 3.0 nm, respectively. The theoretical calculation can explain our experimental results very well, as shown in Fig. 5. Good dispersion and small size of < 2.5 nm

for Pt nanoparticles were found for the 5 wt.%, 10 wt.% and 20 wt.% samples, while the 30 wt.% Pt/SC-CNFs catalyst has some Pt aggregates, because the loading is higher than the

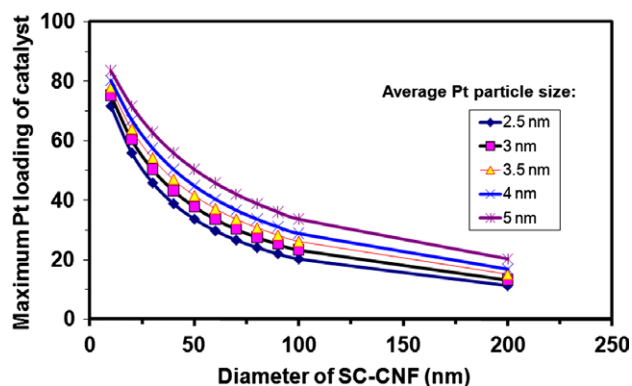


Fig. 5 – Theoretical calculation of CNF's diameter on the maximum possible Pt loading of catalyst based on different average Pt particle size.

maximum of 27 wt.% (plus the mean Pt particle size of 2.9 nm is slightly lower than 3.0 nm). Therefore, choosing smaller diameter CNFs can effectively enlarge the surface area, thus providing larger room for residing Pt nanoparticles.

Fig. 1 shows a schematic illustration of our modified filtration method. Previously, we reported a filtration method for fabricating partially aligned multi-walled carbon nanotubes (MWNTs) based MEA using Nylon filter [36], and the maximum catalyst transfer efficiency is around 60%. In this work, we used polycarbonate filter with a 0.2  $\mu\text{m}$  thickness instead of Nylon filter. Under an optimized hot-press condition, the Pt/SC-CNFs film can be transferred onto the Nafion 112 membrane at nearly 100% transfer efficiency. As evidenced in Fig. 6b, a clean polycarbonate filter after transferring was observed. In contrast, the Nylon filter after transferring still has some Pt/SC-CNFs powders (Fig. 6a), weight difference before

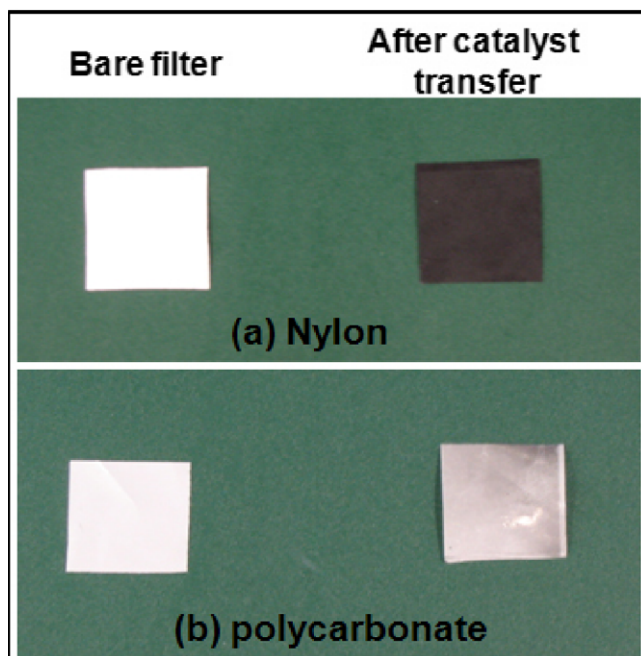


Fig. 6 – Optical pictures of bare filter papers and filter papers after catalysts transferred, (a) Nylon, (b) polycarbonate.

and after transferring catalyst layer shows that it can just achieve a maximum transfer efficiency of 60%.

In our experiment, the cathode and anode catalyst layers coated membranes were obtained before hot-pressing to fabricate the MEAs. The SEM images of the cross-sections of the Pt/SC-CNFs-based CCMs with different Pt loadings in electrodes and catalysts are shown in Fig. 7. It was noticed that the Pt/SC-CNFs layers do not have preferred orientation as previously observed for partially oriented Pt/MWNT cathode film for PEMFC [36]. In the present study, ca. 50 wt.% Nafion® was sprayed during the filtration process and this is probably responsible for the random orientation of the SC-CNFs. Furthermore, the mixed Nafion can help to attain a 100% catalyst transfer because Nafion® makes the Pt/SC-CNFs film more hydrophilic, which is similar to the hydrophilic Nafion membrane, but is different from the hydrophobic nature of polycarbonate filter paper.

At Pt electrode loading of 0.2  $\text{mg}/\text{cm}^2$ , The Pt/SC-CNFs (with catalyst loading of 20 wt.%) catalyst layer is around 15  $\mu\text{m}$  (14.9  $\mu\text{m}$  and 15.8  $\mu\text{m}$ , as shown in Fig. 7d), while at Pt electrode loading of 0.025  $\text{mg}/\text{cm}^2$ , the Pt/SC-CNFs (20 wt.%) catalyst layer is only 3.9  $\mu\text{m}$  (shown in Fig. 7b). With the Pt catalyst loading reducing to 5 wt.%, the Pt/SC-CNFs catalyst with 0.025  $\text{mg}/\text{cm}^2$  electrode loading can form a layer with a thickness of 7.7  $\mu\text{m}$  (Fig. 7c). By using the modified filtration method, the thickness of catalyst layer can be well controlled by altering Pt catalyst loadings and the volumes of Pt/SC-CNFs catalyst inks (determining Pt electrode loading) in the funnel.

Fig. 8 shows the relationship between Pt catalyst loading, Pt electrode loading and catalyst layer thickness based on theoretical calculations. As we have known, higher catalyst loading plus lower electrode Pt metal loading offers thinner catalyst layer. For the 20 wt.% Pt/SC-CNFs catalyst, the thickness of catalyst layer is 3.4  $\mu\text{m}$  at a Pt electrode loading of 0.025  $\text{mg}/\text{cm}^2$ , while the thickness increases to 13.5  $\mu\text{m}$  as the Pt electrode loading increases to 0.2  $\text{mg}/\text{cm}^2$ . However, for a 5 wt.% Pt/SC-CNFs catalyst, the thickness of catalyst layer is 7.6  $\mu\text{m}$ , even at a low Pt metal loading of 0.025  $\text{mg}/\text{cm}^2$ . All these calculations agree with our experimental work very well (compare theoretical calculations with experimental work; see Fig. 7b–d). In the other aspect, it is wise to employ a low Pt loading catalyst (e.g., 5 wt.%) to obtain a uniformly thin anode catalyst layer with low electrode metal loading (e.g., 0.025  $\text{mgPt}/\text{cm}^2$ ), while still keeping a reasonable thickness of catalyst layer. This strategy could effectively prevent 'flooding' in catalyst layer. Therefore, this filtration method offers us a convenient way to prepare the MEAs with different Pt electrode and catalyst loadings, especially ultra-low anode metal loading (e.g., 0.025  $\text{mgPt}/\text{cm}^2$ ), and to test their PEMFC performances.

Fig. 9 shows the  $\text{H}_2/\text{O}_2$ -PEM single cell performances of 4.4- $\text{cm}^2$  Pt/SC-CNFs-based MEAs with anode and cathode loadings varied from 0.2, 0.05 to 0.025  $\text{mgPt}/\text{cm}^2$  and 0.2 to 0.1  $\text{mgPt}/\text{cm}^2$ , respectively. The polarization curves were recorded at 70  $^\circ\text{C}$  under fully humidification at a back pressure of 35 psi. For three MEAs with same cathode structure (20 wt.%, 0.2  $\text{mg}/\text{cm}^2$ ), with the anode Pt loading decreasing from 0.2 to 0.025  $\text{mg}/\text{cm}^2$ , there is no obvious performance difference in the cell voltage at low current region (<0.2  $\text{mA}/\text{cm}^2$ ) observed. However, in the middle and high

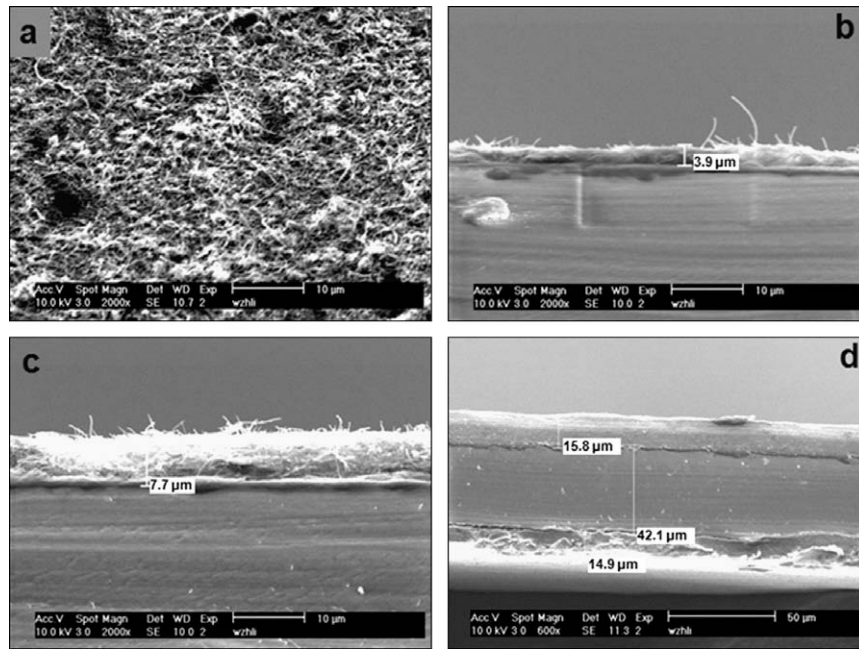


Fig. 7 – SEM images of (a) top view of Pt/SC-CNFs catalyst coated Nafion® 112 membrane, cross-section view of CCM with, (b) cathode layer with 20 wt.%Pt/SC-CNFs, 0.025 mgPt/cm<sup>2</sup>, (c) cathode layer with 5 wt.%Pt/SC-CNFs, 0.025 mgPt/cm<sup>2</sup>, (d) cathode and anode layers with 20 wt.%Pt/SC-CNFs, 0.2 mgPt/cm<sup>2</sup>.

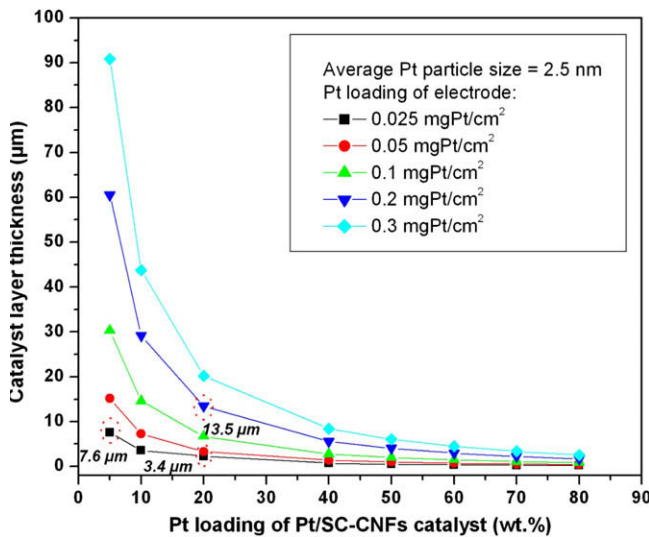


Fig. 8 – Theoretical calculation of catalyst layer thickness (µm) as function of Pt loading of Pt/SC-CNF catalyst (wt.%) and Pt loading of electrode (mgPt/cm<sup>2</sup>).

current density regions, e.g., at current density of 1.0 A/cm<sup>2</sup>, the working voltage difference is about 50 mV, for the MEAs with anode loading deduction from 0.2 to 0.05 mgPt/cm<sup>2</sup>, and from 0.05 to 0.025 mgPt/cm<sup>2</sup>. This value is higher than 30 mV reported for Pt/CB-based MEA [46]. The PEMFC performance decrease is probably attributed to the tube-morphology and high pack density of SC-CNFs. In addition, for two MEAs with electrode and catalyst loadings of 0.05 mgPt/cm<sup>2</sup>, 20 wt.% and 0.025 mgPt/cm<sup>2</sup>, 5 wt.%, more catalytic active sites attributed to higher anode Pt loading (0.05 mg/cm<sup>2</sup> vs.

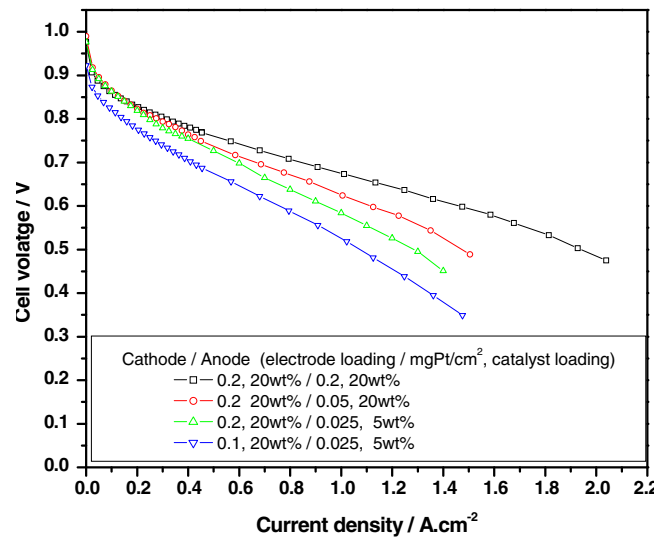
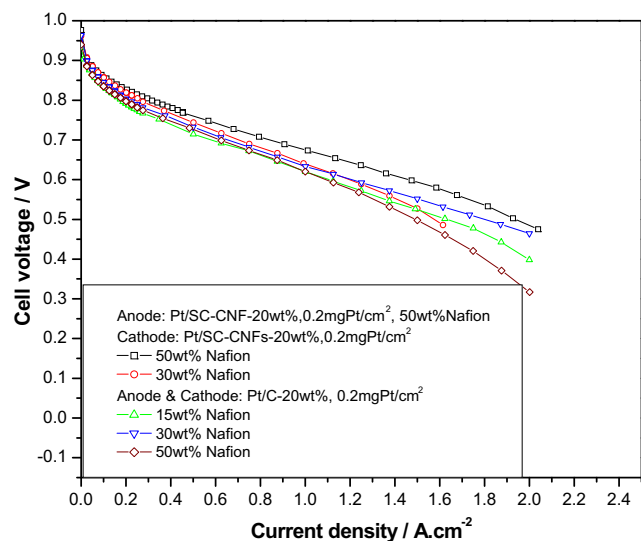


Fig. 9 – PEMFC polarization curves of MEAs with different anode and cathode Pt/SC-CNFs electrode loading and catalyst loading. Test conditions: cell: 70 °C, 100% relative humidity; anode/cathode: H<sub>2</sub>/O<sub>2</sub>, 200/200 mL/min, 35/35 psi.

0.025 mg/cm<sup>2</sup>), and better mass transport attributed to thinner anode catalyst layer (4.4 µm vs. 7.7 µm) will lead to overall PEMFC performance improvement. In contrast, for two MEAs with identical anode structure (0.025 mgPt/cm<sup>2</sup>, 5 wt.%Pt/SC-CNFs), significant PEMFC performance decrease was observed, even at low current density region, with the cathode Pt loading reducing from 0.2 to 0.1 mg/cm<sup>2</sup>: At a working voltage of 0.8 V, the current density reduces almost by half: from 216 mA/cm<sup>2</sup> to 135 mA/cm<sup>2</sup>. It clearly shows the critical





**Fig. 10** – PEMFC polarization curves of MEAs with Pt/C (BASF-Fuel Cell, 20 wt.%) or Pt/SC-CNFs (home-made, 20 wt.%) with different Nafion amount in the cathode. Test conditions: cell: 70 °C, 100% relative humidity; anode/cathode: H<sub>2</sub>/O<sub>2</sub>, 200/200 mL/min, 35/35 psi.

importance of sufficient noble metal loading in the cathode, because the complex four-electron-transfer ORR is sluggish, sufficient Pt loading is a premier factor for an acceptable PEMFC performance.

Fig. 10 shows the PEMFC performance comparison of the MEAs with Pt/C and Pt/SC-CNFs cathode catalysts with different Nafion contents. For the SC-CNFs based MEAs, even the Nafion content is as high as 50 wt.%, the PEMFC performance remains fairly high in all current density regions (the black curve in Fig. 10), while for CB based MEAs, the optimized Nafion amount is around 30 wt.% (the blue curve in Fig. 10), more or less Nafion content in the cathode will result in low PEMFC performance. This is in consistence with our expectation, since CNFs has large aspect (length-to-diameter) ratio, and entangled-tube-morphology, thus, it can make Pt/SC-CNFs more easily form continuously conductive networks in the Nafion matrix than carbon black particle. More Nafion content in the catalyst layer will help to improve the platinum utilization through providing more proton conduction path. Furthermore, SC-CNFs is more hydrophobic than carbon black, therefore, SC-CNFs can improve the mass transport of reactant gas. In our experiments, the peak power density of Pt/SC-CNFs-based MEA can reach around 900 mW/cm<sup>2</sup>, while that of commercial E-TEK based MEA is only 750 mW/cm<sup>2</sup>. More characterization work on the Pt/SC-CNFs-based MEAs needs to carry out to deeply understand the benefits for SC-CNFs.

#### 4. Conclusions

Pt/SC-CNFs films fabricated by the filtration method were investigated as catalyst layers for PEMFC. Using a modified ethylene glycol (EG) method, Pt/SC-CNFs catalysts were successfully prepared with homogeneous Pt particle dispersion (2–4 nm) and uniform particle distribution on the SC-CNFs outer walls. The average Pt particle size and distribution were

found to be strongly dependent on the metal loading of Pt/SC-CNFs at a given nanofiber's diameter. XRD and TEM characterizations show that the Pt particle size increases with metal loading increasing, and the average Pt particle size can be well controlled under 5 nm with a narrow size distribution for low catalyst loading from 5 wt.% to 20 wt.%. Minor Pt agglomerations were observed for Pt/SC-CNFs with 30 wt.%, this is in good agreement with our theoretical calculation that a maximum Pt loading can only reach 27 wt.% for 100 nm diameter SC-CNF supported 3.0 nm Pt nanoparticles. A modified filtration process was employed to fabricate Pt/SC-CNFs catalysts based membrane electrode assembly (MEA), and the catalyst transfer efficiency can reach close to 100% using super-hydrophobic polycarbonate filter. Theoretical calculations can also precisely guide the thickness of the catalyst layer based on the Pt loadings in catalysts and electrodes. The PEM single cell performance of the MEAs using Pt/SC-CNFs with different Pt anode and cathode loadings were tested, and the Pt loading in the cathode was found to be more crucial than that in anode for the PEMFC performance. Pt/SC-CNFs-based MEA demonstrates a higher PEMFC performance than the carbon black (C) based MEA. The optimized Nafion content in the Pt/SC-CNFs-based MEA was found to be around 50 wt.%, which is higher than 30 wt.% for the Pt/C-based MEA. This indicates SC-CNFs can maintain continuous electrical conduction path, which could not be easily cut down by Nafion micelles, attributed to its unique high aspect ratio and entangled morphology, thus, high Pt utilizations can be attained by employing SC-CNFs-based MEAs. This also implies possible reduction in Pt loading of MEA by using SC-CNF support.

#### Acknowledgements

This work is supported by the Pacific Fuel Cell Corp., a UC-Discovery Grant, and the California Energy Commission. We thank Mr. Thanh Nguyen, Dr. Adib Farhad and Mr. Wayne Bosze in Bourns Inc for their kind discussions on the filtration process. W. Li is grateful to the Michigan Technological University Start-Up package D92905.

#### REFERENCES

- [1] Vielstich W, Lamm A, Gasteiger H, editors. Handbook of fuel cells. John Wiley and Sons Inc.; 2004.
- [2] Nørskov JK, Rossmeisl J, Logadottir A, Lindqvist L, Kitchin JR, Bligaard T, et al. Origin of the overpotential for oxygen reduction at a fuel-cell cathode. *J Phys Chem B* 2004;108(46):17886–92.
- [3] Gasteiger HA, Kocha SS, Sompalli B, Wagner FT. Activity benchmarks and requirements for Pt, Pt-alloy, and non-Pt oxygen reduction catalysts for PEMFCs. *Appl Catal B Environ* 2005;56(1–2):9–35.
- [4] Jalan V, Taylor EJ. Importance of interatomic spacing in catalytic reduction of oxygen in phosphoric-acid. *J Electrochem Soc* 1983;130(11):2299–301.
- [5] Mukerjee S, Srinivasan S, Soriaga MP, Mcbreen J. Role of Structural and electronic-properties of Pt and Pt alloys on electrocatalysis of oxygen reduction – an in situ XANES and EXAFS investigation. *J Electrochem Soc* 1995;142(5):1409–22.



- [6] Toda T, Igarashi H, Uchida H, Watanabe M. Enhanced of the electroreduction of oxygen on Pt alloys with Fe, Ni, and Co. *J Electrochem Soc* 1999;146(10):3750–6.
- [7] Ralph TR, Hogarth MP. Catalysis for low temperature fuel cells. Part 1: the cathode challenges. *Platinum Met Rev* 2002;46(1):3–14.
- [8] Paulus UA, Wokaun A, Scherer GG, Schmidt TJ, Stamenkovic V, Radmilovic V, et al. Oxygen reduction on carbon-supported Pt-Ni and Pt-Co alloy catalysts. *J Phys Chem B* 2002;106:4181–91.
- [9] Stamenkovic V, Schmidt TJ, Ross PN, Markovic NM. Surface composition effects in electrocatalysis: kinetics of oxygen reduction on well defined Pt<sub>3</sub>Ni and Pt<sub>3</sub>Co alloy surfaces. *J Phys Chem B* 2002;106(46):11970–9.
- [10] Stamenkovic V, Fowler B, Mun BS, Wang GF, Ross PN, Lucas CA, et al. Improved oxygen reduction activity on Pt<sub>3</sub>Ni(1 1 1) via increased surface site availability. *Science* 2007;315(5811):493–7.
- [11] Li W, Zhou W, Zhou Z, Li H, Zhou B, Zhou B, et al. Nanostructured Pt-Fe/C as cathode catalyst in direct methanol fuel cell. *Electrochim Acta* 2004;49:1045–55.
- [12] Wang B. Recent development of non-platinum catalysts for oxygen reduction reaction. *J Power Sources* 2005;152(1):1–15.
- [13] Sun GQ, Wang JT, Savinell RF. Iron tetramethoxyphenylporphyrin (FeTMPP) as methanol tolerant electrocatalyst for oxygen reduction in direct methanol fuel cells. *J Appl Electrochem* 1998;28(10):1087–93.
- [14] Chu D, Jiang RZ. Novel electrocatalysts for direct methanol fuel cells. *Solid State Ionics* 2002;148(3–4):591–9.
- [15] Marcotte S, Villers D, Guillet N, Roue L, Dodelet JP. Electroreduction of oxygen on Co-based catalysts: determination of the parameters affecting the two-electron transfer reaction in an acid medium. *Electrochim Acta* 2004;50(1):179–88.
- [16] Medard C, Lefevre M, Dodelet JP, Jaouen F, Lindbergh G. Oxygen reduction by Fe-based catalysts in PEM fuel cell conditions: activity and selectivity of the catalysts obtained with two Fe precursors and various carbon supports. *Electrochim Acta* 2006;51(16):3202–13.
- [17] Zhong HX, Zhang HM, Liu G, Liang YM, Hu JW, Yi BL. A novel non-noble electrocatalyst for PEM fuel cell based on molybdenum nitride. *Electrochem Commun* 2006;8(5):707–12.
- [18] Reeve RW, Christensen PA, Hamnett A, Haydock SA, Roy SC. Methanol tolerant oxygen reduction catalysts based on transition metal sulfides. *J Electrochem Soc* 1998;145(10):3463–71.
- [19] Ozenler SS, Kadirgan F. The effect of the matrix on the electro-catalytic properties of methanol tolerant oxygen reduction catalysts based on ruthenium-chalcogenides. *J Power Sources* 2006;154(2):364–9.
- [20] Bashyam R, Zelenay P. A class of non-precious metal composite catalysts for fuel cells. *Nature* 2007;443(7107):63–6.
- [21] Lefevre M, Proietti E, Jaouen F, Dodelet JP. Iron-based catalysts with improved oxygen reduction activity in polymer electrolyte fuel cells. *Science* 2009;324:71–4.
- [22] Gong KP, Du F, Xia ZH, Durstock M, Dai LM. Nitrogen-doped carbon nanotube arrays with high electrocatalytic activity for oxygen reduction. *Science* 2009;323:760–4.
- [23] Che GL, Laksmi BB, Fisher ER, Martin CR. Carbon nanotubule membrane for electrochemical energy storage and production. *Nature* 1998;393(6683):346–9.
- [24] Joo SH, Choi SJ, Oh I, Kwak J, Liu Z, Terasaki O, et al. Ordered nanoporous arrays of carbon supporting high dispersions of platinum nanoparticles. *Nature* 2001;414(6862):470–2.
- [25] Bessel C, Lauberndts K, Rodriguez N, Baker R. Graphite nanofibers as an electrode for fuel cell applications. *J Phys Chem B* 2001;105(6):1115–8.
- [26] Li W, Liang C, Qiu J, Zhou W, Han H, Wei Z, et al. Carbon nanotubes as support for cathode catalyst of a direct methanol fuel cell. *Carbon* 2002;40(5):791–4.
- [27] Liu ZL, Lin XH, Lee JY, Zhang W, Han M, Gan LM. Preparation and characterization of platinum-based electrocatalysts on multiwalled carbon nanotubes for proton exchange membrane fuel cells. *Langmuir* 2002;18(10):4054–60.
- [28] Yoshitake T, Shimakawa Y, Kuroshima S, Kimura H, Ichihashi T, Kubo Y, et al. Preparation of fine platinum catalyst supported on single-wall carbon nanohorns for fuel cell application. *Physica B-Condens Matter* 2002;323(1–4):124–6.
- [29] Li W, Liang C, Zhou W, Qiu J, Zhou Z, Sun G, et al. Preparation and characterization of multiwalled carbon nanotube-supported platinum for cathode catalysts of direct methanol fuel cells. *J Phys Chem B* 2003;107(26):6292–9.
- [30] Wang C, Waje M, Wang X, Tang J, Haddon R, Yan Y. Proton exchange membrane fuel cells with carbon nanotube based electrodes. *Nano Lett* 2004;4(2):345–8.
- [31] Park KW, Sung YE, Han S, Yun Y, Hyeon T. Origin of the enhanced catalytic activity of carbon nanocoil-supported PtRu alloy electrocatalysts. *J Phys Chem B* 2004;108(3):939–44.
- [32] Girishkumar G, Vinodgopal K, Kamat PV. Carbon nanostructures in portable fuel cells: single-walled carbon nanotube electrodes for methanol oxidation and oxygen reduction. *J Phys Chem B* 2004;108(52):19960–6.
- [33] Matsumoto T, Komatsu T, Arai K, Yamazaki T, Kijima M, Shimizu H, et al. Reduction of Pt usage in fuel cell electrocatalysts with carbon nanotubes. *Chem Commun* 2004;7:840–1.
- [34] Kim C, Kim YJ, Kim YA, Yanagisawa T, Park KC, Endo M, et al. *J Appl Phys* 2004;96:5903–5.
- [35] Wang X, Waje M, Yan Y. CNT-based electrodes with high efficiency for PEMFCs. *Electrochem Solid State Lett* 2005;8(1):A42–4.
- [36] Li W, Wang X, Chen Z, Waje M, Yan Y. Carbon nanotube film by filtration as cathode catalyst support for proton-exchange membrane fuel cell. *Langmuir* 2005;21(21):9386–9.
- [37] Waje MM, Wang X, Li W, Yan Y. Deposition of platinum nanoparticles on organic functionalized carbon nanotubes grown in situ on carbon paper for fuel cells. *Nanotechnology* 2005;16(7):S395–400.
- [38] Wang X, Li W, Chen Z, Waje M, Yan Y. Durability investigation of carbon nanotube as catalyst support for proton exchange membrane fuel cell. *J. Power Sources* 2006;158(1):154–9.
- [39] Knupp LS, Li W, Paschos O, Murray TM, Snyder J, Haldar P. The effect of experimental parameters on the synthesis of carbon nanotube/nanofiber supported platinum by polyol processing techniques. *Carbon* 2008;46:1276–84.
- [40] Li W, Yan Y. Pt/SC-CNFs as electrocatalysts for PEMFC, oral presentation, ECS annual meeting at Denver, CO; 2006.
- [41] Iijima S. Helical microtubules of graphite carbon. *Nature* 1992;354(6348):56–8.
- [42] Jorio A, Dresselhaus G, Dresselhaus MS. Carbon nanotubes: advanced topics in the synthesis, structure, properties and applications. Springer-Verlag Heidelberg; 2008.
- [43] De Long KP, Genus JW. Carbon nanofibers: catalytic synthesis and applications. *Catal Rev Sci Eng* 2000;42:481–510.
- [44] Melechko AV, Merkulov VI, McKnight TE, Guillorn MA, Klein KL, Lowndes DH, et al. Vertically aligned carbon nanofibers and related structures: controlled synthesis and directed assembly. *J Appl Phys* 2005;97(4):041301-1–041301-39.
- [45] Endo M, Kim YA, Ezaka M, Osada K, Yanagisawa T, Hayashi T, et al. Selective and efficient impregnation of metal nanoparticles on cup-stacked-type carbon nanofibers. *Nano Lett* 2003;3:723–6.
- [46] Gasteiger HA, Panels JE, Yan SG. Dependence of PEM fuel cell performance on catalyst loading. *J Power Sources* 2004;127(1–2):162–71.